Atom-Bond Electronegativity Equalization Method Fused into Molecular Mechanics. II. A Seven-Site Fluctuating Charge and Flexible Body Water Potential Function for Liquid Water

Yang Wu and Zhong-Zhi Yang*

Department of Chemistry, Liaoning Normal University, Dalian 116029, People's Republic of China

Received: February 10, 2004; In Final Form: May 19, 2004

The ABEEM-7P model, which is a transferable, intermolecular-potential seven-points approach including fluctuating charges and flexible body, is based on the combination of the atom-bond electronegativity equalization (ABEEM) and molecular mechanics (MM). This model has been successfully explored in regard to the properties of gas-phase small water clusters in reasonable agreement with available experiments and other water models. This model is further tested by comparing the calculated energetic, structural, and dynamic properties of liquid water over a range of temperatures (260−348 K) with available experimental results and those from other water models. Molecular dynamics simulations of liquid water with ABEEM-7P were performed using the Tinker MM program. All simulations were conducted in the microcanonical NVE ensemble or canonical NVT ensemble, using 216 water molecules in a cubic simulation cell furnished with periodic boundary and minimum image conditions, and the density of the solvent was set to the experimental value for the temperature of interest. The ABEEM-7P potential gives a reasonable experimental reproduction of the intramolecular O−H bond length and H−O−H bond angle in the liquid at room temperature. The ABEEM-7P model presents the quantitative charges of O atoms, H atoms, O−H bonds, and lone-pair electrons per monomer water in the liquid and their changing in response to different ambient environment from 260 K to 348 K. Especially, ABEEM-7P applies the parameter $k_{lp,H}(R_{lp,H})$ to explicitly describe short-range interaction of the hydrogen bond in the hydrogen-bond interaction region. The computed ABEEM-7P properties of the liquid-phase water at room temperature, such as average dipole moment, static dielectric constant, heats of vaporization, radial distribution function, and diffusion constant, are fairly consistent with the available experimental results. The ABEEM-7P model also performs well for the temperature dependence of liquid properties: the static dielectric constant and the heats of vaporization by ABEEM-7P decrease as the temperature increases, in good agreement with the experimental values.

1. Introduction

The structural investigation of water has strong historical precedence; its roots trace at least as far back as Roentgen's early work on the structure of water and the explanation of its density maximum[1] and Bernal and Fowler's model of hydrogen-bonding structure in the liquid.[2] In principle, an accurate characterization of the molecular structure of liquid water can be found from solution scattering experiments. The X-ray scattering studies of Narten and Levy[3] and the neutron diffraction experiments conducted by Soper and co-workers[4−7] are commonly cited as the definitive sources for the radial distribution function (g_{OO}, g_{HH}, g_{OH}) of liquid water. Neutron diffraction with isotopic substitutions (NDIS) has been used to measure intermolecular partial pair correlation functions for liquid water.[4−8] The self-diffusion coefficient of pure water has been measured to be 2.3×10^{-9} m^2/s at 298 K, using the diaphragm-cell technique[9] or the pulsed-gradient spin−echo (PGSE) NMR method.[10] Simultaneously, several theoretical methods have been developed to give more-explicit considerations of the properties of liquid water. Ab initio molecular dynamics (MD)[11−13] is free from any approximations of empirical parametrization. Because of the computational requirements of the ab initio models, their application has been limited, so far, to small systems and short times; however, they have provided a wealth of information about water.

A critical component in the theoretical research involves the intermolecular potentials that describe the interactions between monomers in the fluids. Simple point-charge models[14−25] such as SPC,[15] SPC/E,[17] TIP3P, TIP4P,[16] and TIP5P[20,21] are now used widely as condensed phase potentials in computer simulations of energetic and structural properties of water. These rigid nonpolarizable models use fixed charges that must reflect average or mean field-charge values for the particular phase and have limited transferability to other thermodynamic states and may exhibit problems in mixtures with ions or nonpolar species, because the electronic configuration of a given water molecule should be dependent explicitly on its environment. For example, the monomer dipole moment from its isolated gas-phase value[26] of 1.85 D is enhanced to the generally accepted value[27,28] of 2.6 D for a water molecule in the ice Ih. There is a considerable controversy on the exact value of the average molecular dipole moment in condensed phases, and, recently, a value of ∼3.0 D has been reported for liquid and solid phases of water.[12,28−30]

Polarizable empirical force fields are "effective" potentials that reflect the response of the electron density to an electrostatic field. For molecules, such a response is sorted into two effects:

* Author to whom correspondence should be addressed. Telephone: 86-411-4259607. E-mail address: zzyang@lnnu.edu.cn.

10.1021/jp0493881 CCC: $27.50
Published on Web 08/21/2004

the local density distortions or responses around a given atom, and electron transfers from atom to surrounding atoms or bonds within the same molecule. Dipole polarizable models are constructed to treat the first effect,[31−44] whereas fluctuating charge models treat the second effect.[45−55] Another model allows for charges to move between any charged sites such as atoms, bonds, and lone-pair electrons.[55] Other models combine both inducible dipoles and fluctuating charges.[56−58] Polarizable dipoles describe the induction effect, whereby the electric field caused by other atoms and molecules polarizes an atom center, which, in turn, produces an electric field that affects neighboring centers and their fields. More-recent activity has involved the development of fluctuating charge models, which have polarizability to all orders in the charge moments and not only the dipole polarizability, compared with dipole polarizable models. The fluctuating charge force fields are based on the electronegativity equalization method (EEM)[59−64] and the recently devised atom-bond electronegativity equalization method (ABEEM),[65−69] both sourced in the context of density functional theory (DFT).[70−72] The widely used fluctuating charge models of treating the water system were reported by Rick et al.;[47] these models are called TIP4P-FQ and SPC-FQ, using the TIP4P and SPC water geometries, and the TIP4P-FQ model gave better results for various properties.

Another attempt to improve potential functions for liquid water is the addition of molecular flexibility,[18,23,45,75−86] i.e., allowing the O−H bond lengths and H−O−H bond angles to vibrate. An earlier novel flexible water model was pioneered by Stillinger and Rahman;[75] this model allowed the H atom to dissociate in the liquid. The model reproduced the water structure but gave a diffusion rate that was too small. The diffusion properties of water seem to be dependent on the internal flexibility; however, there is disagreement about whether flexibility increases[77] or decreases[79,80] the diffusion constant. Several studies of flexible three-point water models[18,23,76−78] found that flexibility did not increase the tetrahedral structure, whereas, in other simulations, flexibility did lead to a more-tetrahedral structure.[3,36] Lately, Stern and Berne[45] performed path-integral MD simulations of a flexible, polarizable water model that was parametrized from ab initio calculations. Their computed results demonstrated that the distributions of O−H bond lengths and H−O−H angles in liquid phase were in agreement with experimental measurements[85,86] and other previous reported flexible models.[79,82,83] Conceptually, because of the increasing electric field experienced by the water molecule, the O−H bond length stretches and the H−O−H bond angle decreases in value, to give a larger dipole moment. Although rigid water is still used most commonly in simulations of different systems, including liquid water and macromolecules in solution, an increasing number of recent simulations do include internal flexibility.[18,23,45]

Lately, Yang, Wu, and Zhao[55] reported a new water model: a transferable, intermolecular, seven-point approach including fluctuation charges and flexible body (ABEEM-7P), which coupled the fluctuating partial charges calculated by atom-bond electronegativity equalization method (ABEEM) developed by Yang and co-workers[65−69] and molecular mechanics (MM). The ABEEM-7P model uses a slightly complicated tetrahedral geometry that is similar to that with the TIP5P model and introduces additional interaction sites, atoms, bonds, and lone-pair electrons, to describe the charge in more detail, i.e., there are seven charged points (three atoms, two bonds, and two lone-pair electrons) in monomer water, all of which are fluctuating with changing environments. In addition, the ABEEM-7P model introduces molecular flexibility, which will analyze the vibration of bond lengths and angles and allow the evaluation of intramolecular interactions. Such improvements have been desirable to develop models with increasing accuracy,[22] and the ABEEM-7P force field has reproduced several gas-phase properties of water clusters $(H_2O)_n$ $(n = 1-6)$[55] that are in reasonable agreement with those measured using available experiments and ab initio calculations.

In this study, we will continue to develop the ABEEM-7P model to simulate the large-scale condensed phase properties by MD simulations and compare the data with available experimental results. This paper is organized as follows. Section II describes the ABEEM-7P model in general form, as well its specific application to liquid water. Section III is devoted to the computational details of simulation procedure. Section IV presents the results of the computation and discussion. Finally, a brief conclusion and outlook to future applications are given.

2. ABEEM-7P Model

The nonrigid body and fluctuating charge model, which is a transferable, intermolecular, seven-point approach (ABEEM-7P), is introduced by Yang, Wu, and Zhao,[55] in which the bond and angle are allowed to vibrate and the partial charges on charged sites are treated to response to changes in their environments. The ABEEM-7P model uses the combination of the atom-bond electronegativity equalization and molecular mechanics (ABEEM/MM).

Atom-bond electronegativity equalization method (ABEEM)[65−69] has been developed by Yang and co-workers in the framework of density function theory and successfully applied to compute charge and energy of a single organic or biological macromolecule. When extending the ABEEM model to a system containing many molecules, such as a water system, special attention must be given to the description of the intermolecular potential energy surface (IPS). In the water system, many of the special properties are due to the ability of water molecules to form hydrogen bonds with other water molecules; thus, correct description of the hydrogen bond is essential to IPS. Yang, Wu, and Zhao[55] have introduced a "hydrogen bond interaction region (HBIR)", in which the interaction between the lone-pair electron of the O atom of one water molecule and the H atom of the other is dependent on their distance until the hydrogen bond is formed, and they have used a new fitted function $k_{lp,H}(R_{lp,H})$ that was extracted from the initial ABEEM overall correction coefficient k[65−69] to describe the electrostatic interaction of the intermolecular hydrogen bond in the HBIR effectively. The total energy expression of the ABEEM for a water system is written as eq 1:

$$E_{\mathrm{ABEEM}} = \sum_{i=1}^{N_{\mathrm{mol}}} \Bigg\{ \sum_{a} [E^*_{ia} - \mu^*_{ia} q_{ia} + \eta^*_{ia} q^2_{ia}] + \sum_{lp} [E^*_{i(lp)} - \mu^*_{i(lp)} q_{i(lp)} + \eta^*_{i(lp)} q_{i(lp)}{}^2] + \sum_{a-b} [E^*_{i(a-b)} - \mu^*_{i(a-b)} q_{i(a-b)} + \eta^*_{i(a-b)} q^2_{i(a-b)}] + \sum_{g-h} \sum_{a(=g,h)} \frac{k_{ia,i(g-h)} q_{ia} q_{i(g-h)}}{R_{ia,i(g-h)}} + \sum_{a} \sum_{lp(\in a)} \frac{k_{ia,i(lp)} q_{ia} q_{i(lp)}}{R_{ia,i(lp)}} +$$

$$k\left[\frac{1}{2}\sum_{a}\sum_{b(\neq a)}\frac{q_{ia}q_{ib}}{R_{ia,ib}}+\frac{1}{2}\sum_{a-b}\sum_{g-h(\neq a-b)}\frac{q_{i(a-b)}q_{i(g-h)}}{R_{i(a-b),i(g-h)}}+\right.$$
$$\frac{1}{2}\sum_{lp}\sum_{lp'(\neq lp)}\frac{q_{i(lp)}q_{i(lp')}}{R_{i(lp),i(lp')}}+\sum_{g-h}\sum_{a(\neq g,h)}\frac{q_{ia}q_{i(g-h)}}{R_{ia,i(g-h)}}+$$
$$\left.\sum_{a}\sum_{lp(\notin a)}\frac{q_{ia}q_{i(lp)}}{R_{ia,i(lp)}}+\sum_{lp}\sum_{a-b}\frac{q_{i(a-b)}q_{i(lp)}}{R_{i(a-b),i(lp)}}\right]\Bigg\}+$$
$$\sum_{i=1}^{N_{\mathrm{mol}}}\sum_{j=1(\neq i)}^{N_{\mathrm{mol}}}\Bigg\{\sum_{\substack{\mathrm{H}\in i\\ (H,lp\text{ in HBIR})}}\sum_{lp\in j}k_{lp,\mathrm{H}}(R_{i\mathrm{H},j(lp)})\frac{q_{i\mathrm{H}}q_{j(lp)}}{R_{i\mathrm{H},j(lp)}}+$$
$$k\Bigg[\frac{1}{2}\sum_{a}\sum_{b}\frac{q_{ia}q_{jb}}{R_{ia,jb}}+\frac{1}{2}\sum_{a-b}\sum_{g-h}\frac{q_{i(a-b)}q_{j(g-h)}}{R_{i(a-b),j(g-h)}}+$$
$$\frac{1}{2}\sum_{lp}\sum_{lp'}\frac{q_{i(lp)}q_{j(lp')}}{R_{i(lp),j(lp')}}+\sum_{g-h}\sum_{a}\frac{q_{ia}q_{j(g-h)}}{R_{ia,j(g-h)}}+$$
$$\left.\sum_{\substack{a\\ (a\neq\mathrm{H},\mathrm{H}\text{ in HBIR}\\ \text{and }lp\text{ not in HBIR})}}\sum_{lp}\frac{q_{ia}q_{j(lp)}}{R_{ia,j(lp)}}+\sum_{lp}\sum_{a-b}\frac{q_{i(a-b)}q_{j(lp)}}{R_{i(a-b),j(lp)}}\right]\Bigg\}\quad(1)$$

where N_{mol} represents the number of water molecules in the system, and the summation covers all water molecules; μ^*_{ia}, η^*_{ia}, and q_{ia} are the valence-state chemical potential, the valence-state hardness, and the partial charge of atom a in molecule i, respectively; $\mu^*_{i(a-b)}$, $\eta^*_{i(a-b)}$, and $q_{i(a-b)}$ are the valence-state chemical potential, the valence-state hardness, and partial charge of bond $a-b$ in molecule i, respectively; and $\mu^*_{i(lp)}$, $\eta^*_{i(lp)}$, and $q_{i(lp)}$ are the valence-state chemical potential, the valence-state hardness, and the partial charge of lone-pair electron lp in molecule i, respectively. It is easy to see that the first term in eq 1 represents the intramolecular energy for water molecules, whereas the second term represents the intermolecular interaction energy between water molecules. The parameter k is an overall correction coefficient that is similar to that previously reported in the ABEEM papers[65−69] and is same both in the first and second term, and $k_{lp,\mathrm{H}}(R_{i\mathrm{H},jlp})$ is related to the separation between the H atom belonging to molecule i and the lone-pair electron belonging to molecule j in the hydrogen-bond interaction region (HBIR).[55]

The existence of a unique chemical potential everywhere in the molecule establishes the electronegativity equalization principle.[70,72−74] The effective electronegativity χ of atom a, bond $a-b$, and lone-pair electron lp in molecule i is now defined using eq 1, according to its formalism by means of density functional theory, as the negative of the corresponding chemical potential μ, i.e., the partial derivative of the total energy E, with respect to the corresponding electron number or partial charge:

$$\chi_a=-\mu_a=-\left(\frac{\partial E}{\partial N_a}\right)_{R,Na}=\left(\frac{\partial E}{\partial q_a}\right)_{R,qa}$$

where χ_a is the corresponding electronegativity for atom a (same for the bond and lone-pair electron) in the conceptual density functional theory. Thus, we can obtain eq 2 for the effective electronegativity of atom a, bond $a-b$, and lone-pair electron lp in water molecule i, respectively:

$$\chi_{ia}=\chi^*_{ia}+2\eta^*_{ia}q_{ia}+C_{ia}\Big(\sum_{a-b}q_{i(a-b)}+\sum_{lp(\in a)}q_{i(lp)}\Big)+$$
$$k\left(\sum_{b(\neq a)}\frac{q_{ib}}{R_{ia,ib}}+\sum_{g-h(\neq a-b)}\frac{q_{i(g-h)}}{R_{ia,i(g-h)}}+\sum_{lp(\notin a)}\frac{q_{i(lp)}}{R_{ia,i(lp)}}\right)+$$
$$\sum_{j\neq i}\Bigg[\sum_{\substack{lp\\ a=\mathrm{H}\\ \mathrm{H,lp\text{ in HBIR}}}}k_{lp,H}(R_{ia,jlp})\frac{q_{lp}}{R_{ia,jlp}}+$$
$$k\left(\sum_{b}\frac{q_{jb}}{R_{ia,jb}}+\sum_{g-h}\frac{q_{j(g-h)}}{R_{ia,j(g-h)}}+\sum_{\substack{lp\\ lp\text{ not in HBIR}}}\frac{q_{j(lp)}}{R_{ia,j(lp)}}\right)\Bigg]\quad(2a)$$

$$\chi_{i(a-b)}=\chi^*_{i(a-b)}+2\eta^*_{i(a-b)}q_{i(a-b)}+C_{i(a-b),ia}q_a+$$
$$D_{i(a-b),ib}q_{ib}+k\left(\sum_{g(\neq a,b)}\frac{q_{ig}}{R_{i(a-b),ig}}+\sum_{g-h(\neq a-b)}\frac{q_{i(g-h)}}{R_{i(a-b),i(g-h)}}+\right.$$
$$\left.\sum_{lp}\frac{q_{i(lp)}}{R_{i(a-b),i(lp)}}\right)+k\sum_{j\neq i}\left(\sum_{g}\frac{q_{jg}}{R_{i(a-b),jg}}+\sum_{g-h(\neq a-b)}\frac{q_{j(g-h)}}{R_{i(a-b),j(g-h)}}+\right.$$
$$\left.\sum_{lp}\frac{q_{j(lp)}}{R_{i(a-b),j(lp)}}\right)\quad(2b)$$

$$\chi_{i(lp)}=\chi^*_{i(lp)}+2\eta^*_{i(lp)}q_{i(lp)}+C_{i(lp)}q_{ia[\in i(lp)]}+$$
$$k\left(\sum_{g(\notin lp)}\frac{q_{ig}}{R_{i(lp),ig}}+\sum_{g-h}\frac{q_{i(g-h)}}{R_{i(lp),i(g-h)}}+\sum_{lp'(\neq lp)}\frac{q_{i(lp')}}{R_{i(lp'),i(lp)}}\right)+$$
$$\sum_{j\neq i}\Bigg[\sum_{\substack{a\\ a=\mathrm{H}\\ \mathrm{H,lp\text{ in HBIR}}}}k_{lp,\mathrm{H}}(R_{ia,jlp})\frac{q_{lp}}{R_{ia,jlp}}+$$
$$k\left(\sum_{\substack{g\\ g\neq\mathrm{H}\\ (\mathrm{H\text{ in HBIR}})}}\frac{q_{jg}}{R_{i(lp),jg}}+\sum_{g-h}\frac{q_{j(g-h)}}{R_{i(lp),j(g-h)}}+\sum_{lp'}\frac{q_{j(lp')}}{R_{j(lp'),i(lp)}}\right)\Bigg]\quad(2c)$$

in which $\chi^*_{ia}=-\mu^*_{ia}$, $\chi^*_{i(a-b)}=-\mu^*_{i(a-b)}$, and $\chi^*_{i(lp)}=-\mu^*_{i(lp)}$ are the valence-state electronegativities of atom a, bond $a-b$, and lone-pair electron lp in molecule i, respectively. $C_{i(a-b),ia}=k_{ia,i(a-b)}/R_{ia,i(a-b)}$, $D_{i(a-b),ib}=k_{ib,i(a-b)}/R_{ib,I(a-b)}$, C_{ia}, and $C_{i(lp)}$ are regarded as adjustable parameters.

For a system of many molecules, the charges also are not independent variables, because there is a charge conservation constraint. For uncharged molecular systems, the constraint can be of two types:

(1) The entire system is constrained to be neutral, so individual molecules can carry a nonzero charge, because there can be intermolecular charge transfer. In addition, the corresponding chemical potentials of all the atoms, bonds, and lone-pair electrons of the system will be equal. As a result, there is only one charge constraint equation and one electronegativity equalization equation of the entire system.

(2) Each molecule is constrained to be neutral, so there is no intermolecular charge transfer, and the chemical potentials of an atom, a bond, and a lone-pair electron will only be equal within a molecule. Therefore, there are N_{mol} charge constraint functions and N_{mol} electronegativity equalization functions. The details have been explicitly described in the literature.[55,65−69]

Generally, force fields used in molecular mechanics (MM) calculations describe the potential energy E of the water system, written as a sum of the intramolecular vibration energy, the van der Waals (vdW) dispersion energy, and the electrostatic interaction energy. The total energy of the ABEEM-7P model, based on the combination of the ABEEM and MM (ABEEM/MM), can be expressed as follows:

$$E_{\mathrm{ABEEM/MM}} = \sum_{\text{bonds}} D[\mathrm{e}^{-2\alpha(r-r_{\mathrm{eq}})} - 2\mathrm{e}^{-\alpha(r-r_{\mathrm{eq}})}] + \sum_{\text{angles}} f_\theta(\theta-\theta_{\mathrm{eq}}) + \sum_i \sum_{j\neq i} \left\{ \sum_a \sum_b \epsilon_{ia,jb} \left[\left(\frac{r_{\min\, ia,jb}}{r_{ia,jb}} \right)^{12} - 2\left(\frac{r_{\min\, ia,jb}}{r_{ia,jb}} \right)^{6} \right] + \sum_{\substack{\mathrm{H}\in i \\ (\mathrm{H},lp \text{ in HBIR})}} \sum_{lp\in j} k_{lp,\mathrm{H}}(R_{i\mathrm{H},j(lp)}) \frac{q_{i\mathrm{H}} q_{j(lp)}}{R_{i\mathrm{H},j(lp)}} + k \left[\frac{1}{2}\sum_a \sum_b \frac{q_{ia}q_{jb}}{R_{ia,jb}} + \frac{1}{2}\sum_{a-b} \sum_{g-h} \frac{q_{i(a-b)}q_{j(g-h)}}{R_{i(a-b),j(g-h)}} + \frac{1}{2}\sum_{lp}\sum_{lp'} \frac{q_{i(lp)}q_{j(lp')}}{R_{i(lp),j(lp')}} + \sum_{g-h}\sum_a \frac{q_{ia}q_{j(g-h)}}{R_{ia,j(g-h)}} + \sum_{\substack{a \\ (a\neq \mathrm{H,H \text{ in HBIR}} \\ \text{and } lp \text{ not in HBIR})}} \sum_{lp} \frac{q_{ia}q_{j(lp)}}{R_{ia,j(lp)}} + \sum_{lp}\sum_{a-b} \frac{q_{i(a-b)}q_{j(lp)}}{R_{i(a-b),j(lp)}} \right] \right\} \quad (3)$$

In the ABEEM-7P model, the Morse potential is chosen for the bond stretching, because it can describe a wide range of behavior from the equilibrium geometry to dissociation, and the harmonic potential is used to describe the angle bending. The Lennard-Jones (LJ) interaction energy between water molecules involves not only vdW parameters for the oxygen−oxygen interactions and hydrogen−hydrogen interactions but also for the oxygen−hydrogen interactions. For the oxygen−hydrogen interaction, the well depth equals the geometric mean of the well depth for the two pure species and the minimum energy distance is given as the arithmetic mean. The electrostatic interaction is the key point of the implementation of ABEEM in MM. The simplest and most consistently used combination of ABEEM and MM is to take the last term of eq 1 into eq 3, that is, to calculate the intermolecular electrostatic interaction (E_{elec}) of eq 3 using the ABEEM charges. In eq 3, D is the dissociation energy of the bond and α is related to the bond force constant ($\alpha = \sqrt{f_b/(2D)}$, where f_b is the bond force constant); r_{eq} is the equilibrium bond length; f_θ is the angle force constant; θ_{eq} is the equilibrium bond angle; $\epsilon_{ia,jb}$ and $r_{\min\, ia,jb}$ are the LJ well depth and minimum energy distance for atoms a and b in molecules i and j, respectively; and q is the charge calculated from the ABEEM method. For the explicit description of the combination of ABEEM and MM and the construction of the ABEEM-7P model, the readers can refer to ref 55.

ABEEM-7P has a tetrahedral geometry for the O atom, similar to the ST2 model of Stillinger and Rahman,[14] the TIP5P model of Mahoney and Jorgensen,[20,21] and the POL5 water potential of Stern et al.[58] The coefficients χ^*, η^*, C, and D of ABEEM and the parameters D, α, f_θ, ϵ, and $r_{\min}$ of MM are adjusted to reproduce properties (structures, dipole moments, energies, vibration frequencies) of the small water clusters because the water trimer, tetramer, pentamer, and hexamer are some of the dominant structures identified in room-temperature liquid water and isomers of the hexamer have a special role in the properties of liquid water and ice.[87,88] In monomer water, the ABEEM-7P model gives the partial positive charges on O and H atoms, which are balanced by appropriate negative charges located around the O−H bonds and the lone-pair electron centers. For two different types of neutrality constraint and electronegativity equalization, ABEEM-7P fits different $k_{lp,\mathrm{H}}(R_{lp,\mathrm{H}})$ functions respectively, to describe the best relationship between the separation of the lone-pair electron and the H atom in HBIR. The method with a charge neutrality constraint and eletronegativity equalization on the entire system is called ABEEM-7P-1, whereas the method with a charge neutrality constraint and eletronegativity equalization on each water molecule is called ABEEM-7P-2. The details of ABEEM-7P parametrization can be found in ref 55.

The ABEEM-7P potential has been successfully applied to accurately reproduce gas-phase state properties of small water clusters $(H_2O)_n$ ($n = 1-6$) and lower energetic isomers (cyclic, cage, book, and prism) of hexamer water,[55] including optimized geometries, monomer dipole moments, vibrational frequencies, cluster interaction energies, and lower energetic conformations of hexamer water, etc. In this study, the properties of liquid water by the ABEEM-7P model over a range of temperature, such as bond length and bond angle, charge distribution, monomer dipole moment, heat of vaporization, static dielectric constant, radial distribution function, and diffusion coefficient, will be examined by MD simulations.

3. Computational Details of Simulation Procedure

All MD runs are performed using the modified Tinker program in the canonical (constant temperature and volume, NVT) ensemble with Berendsen thermostats[90] or in the microcanonical (constant energy and volume, NVE) ensemble with the velocity Verlet integrator. All runs use cubic periodic boundary conditions, 216 water molecules, and a time step of 1 fs. The density of solvent is set to the experimental value for the temperature of interest (260−348 K)[91−93] by adjusting the volume of the box. In the NVT ensemble, the temperature is allowed to vary approximately ±5 K around the desired temperature. Minimum image conditions[94] are used, and, because solvent molecules are explicitly present, no macroscopic dielectric constant is needed. The computer processing unit (CPU) required for simulations with our ABEEM-7P model is an approximate factor of 3.0 larger than for the corresponding fluctuating charge model, such as TIP4P-FQ. For the convenience of computations by the ABEEM-7P potential, several points must be mentioned:

(1) Although the ABEEM-7P water model computes the explicit charges of atoms, bonds, and lone-pair electrons in the water system, the force is only acting on the atoms by the repartition of charges from bonds and lone-pair electrons to atoms. We will try to assign a small charge mass, which is a fictitious quantity, to the sites of bonds and lone-pair electrons, which will be an improved alternative for the ABEEM-7P model in the future. Atoms in the system are randomly assigned

TABLE 1: Properties of the ABEEM-7P Model for Liquid Water, Including the Average Bond Length (r_{OH}), Average Bond Angle (θ_{HOH}), Energy (U_{liquid}), Heat of Vaporization (ΔH_{vap}), Average Dipole Moment (μ), Static Dielectric Constant (ϵ_0), and the Translational Diffusion Constant (D) at Room Temperature (298 K)[a]

	ABEEM-7P	POL5[b]	TIP4P-FQ[c]	TIP5P[d]	MCDHO[e]	experiment
r_{OH} (Å)	0.968 ± 0.002				0.985	0.970[f]
θ_{HOH} (deg)	102.8 ± 0.8				102.79 ± 0.01	106,[g] 102.8[h]
U_{liquid} (kcal/mol)	-10.26 ± 0.08	-9.92 ± 0.01	-9.89 ± 0.02	-9.87 ± 0.01	-10.40 ± 0.01	-9.92[i]
ΔH_{vap} (kcal/mol)	10.85 ± 0.08	10.51 ± 0.01	10.48 ± 0.01	10.46 ± 0.01	10.99 ± 0.01	10.51[i]
μ (D)	2.80 ± 0.01	2.712 ± 0.02	2.6	2.29	3.01 ± 0.01	
ϵ_O	76 ± 1	98 ± 8	79 ± 8	82 ± 2		78.3[j]
D ($\times 10^{-9}$ m^2/s)	1.8 ± 0.1	1.81 ± 0.06	1.9 ± 0.1	2.6 ± 0.04		2.3[k]

[a] Also shown are the available experimental results and other potential values. [b] From ref 58. [c] From refs 47 and 54. [d] From refs 20 and 21. [e] From refs 45 and 83. [f] From ref 85. [g] From intramolecular O−H and H−H distances reported in ref 85. [h] From ref 86. [i] From refs 92 and 97. [j] From refs 102 and 103. [k] From ref 105.

velocities that are appropriate for the temperature of simulation, according to Maxwellian distribution. Atoms are allowed to move according to Newton's equations of motion, and the velocities of atoms are adjusted intermittently until the system reaches the desired temperature.

(2) The cutoff for the nonbonded interactions is 9.0 Å for all simulations and the nonbonded interactions are truncated, using force shifting,[95] where the calculated forces and energies are smoothly shifted to zero at the cutoff distance. This scheme[96] has been observed to give similar structural and dynamic properties for bulk water with those by means of Ewald summation.

(3) The fact that charges are or are not allowed to transfer between different molecules or just between charged sites on the same molecule makes some difference for the two ABEEM-7P models.[55] For the computed properties of gas-phase small water clusters, the ABEEM-7P-2 model, which constrains the charge neutrality and electronegativity equalization on each water molecule, gives better results, to some degree, than those by the ABEEM-7P-1 model, which constrains the charge neutrality and electronegativity equalization on the entire water system, especially for computation of the dimer dipole moment. Therefore, in the present application, we have included a charge neutrality constraint on each water molecule and there is no charge transfer between molecules and the effective chemical potential of an atom, a bond, and a lone-pair electron are to be equal only within a molecule, i.e., the ABEEM-7P-2 model (simply referenced as ABEEM-7P). Rather than solve for the charges exactly at each time step, we recalculate the charges of the atoms, bonds, and lone-pair electrons every picosecond, in consideration of the expensive computational time.

(4) For all molecular dynamics, 100 ps of equilibration is followed by 500-ps simulations (used for calculations of the various properties) and an additional 500-ps trajectory is conducted at <298 K, to ensure the stability of the computed values, which is due to much-slower convergence at low temperature.[20]

4. Results and Discussions

In this section, we present the results and discussions from our MD simulations on several properties such as bond length and bond angle, charge distribution, monomer dipole moment, heat of vaporization, static dielectric constant, radial distribution function, and diffusion coefficient for liquid water at a range of temperatures (260−348 K) by means of the ABEEM-7P force field. We make comparisons with the available experimental data and also compare the results with other water potentials that have been reported in the literature, including those from the TIP5P potential of Mahoney and Jorgensen et al.[20,21] (an empirical fixed charge force field with five interaction sites located on the O atom, two H atoms, and two lone-pair electrons), the TIP4P−FQ potential of Rick, Stuart, and Berne[47,54] (an empirical polarizable model with fluctuating charges), the POL5 potential of Stern et al.[58] (an ab initio model including polarizable electrostatics based on the combination of the fluctuating bond-charge increments and the polarizable dipoles); and the MCDHO potential of Saint-Martin et al.[45,83] (a flexible, polarizable water model parametrized from the ab initio calculations).

4.1. Liquid Water at Room Temperature and Pressure. 4.1.1. Bond Length and Bond Angle. Table 1 summarizes the liquid-state properties computed at room temperature from MD simulations. The ABEEM-7P water model presents the O−H stretching via a Morse function, which is similar to the MCDHO water model,[45,83] and the H−O−H bending by a harmonic potential, whereas the MCDHO model used a quartic polynomial.[45,83] The computed average bond length in the liquid state, using the ABEEM-7P model, is 0.968 Å, in excellent agreement with recent experimental measurement (0.970 Å),[85] and the corresponding value of the flexible, polarizable MCDHO water model was 0.985 Å. For both flexible force field models (MCDHO and ABEEM-7P) and experiments, the average value of bond length is shifted toward longer length in the liquid phase. However, both ABEEM-7P and MCDHO simulations show a shift toward smaller H−O−H angles in the liquid phase (the average angle by ABEEM-7P and MCDHO is 102.8° and 102.79°, respectively), in contrast with the larger angle deduced from experimental measurements of the intramolecular H−H distance.[85] This discrepancy seems to be common, because the H−O−H angle for many other flexible water models also grows smaller upon solvation.[45,79,82,83] Note that an earlier reference[86] reported an experimental angle in the liquid (102.8°) that was also smaller than the gas-phase value and very close to the value determined by the ABEEM-7P and MCDHO models. Although the H−O−H angle in the liquid phase, as determined by the ABEEM-7P model, is smaller than the gas-phase monomer angle, ABEEM-7P predicted a slight increase in the average bend angle in gas-phase water clusters $(H_2O)_n$ ($n = 2-6$). The average angle of dimmer and cyclic $(H_2O)_n$ ($n = 3, 4, 5, 6$) is 105.06°, 106.15°, 105.73°, 105.94°, and 106.64°, respectively, and the corresponding value of hexamer isomers (book, prism, cage) is 105.28°, 105.22°, and 105.01°, respectively, all of which are larger than the gas-phase monomer angle of 104.52° and are in agreement with the ab initio results.[84] A change in the angle upon solvation is likely, because of at least two competing effects.[45] Polarization from surrounding molecules induces a larger dipole moment and, thus, should be associated with a smaller angle. However, the constraint of (partial) tetrahedral ordering should induce a larger angle closer to the tetrahedral angle (109.47°). In addition, Burnham and Xantheas recently suggested that the most probable reason some models could

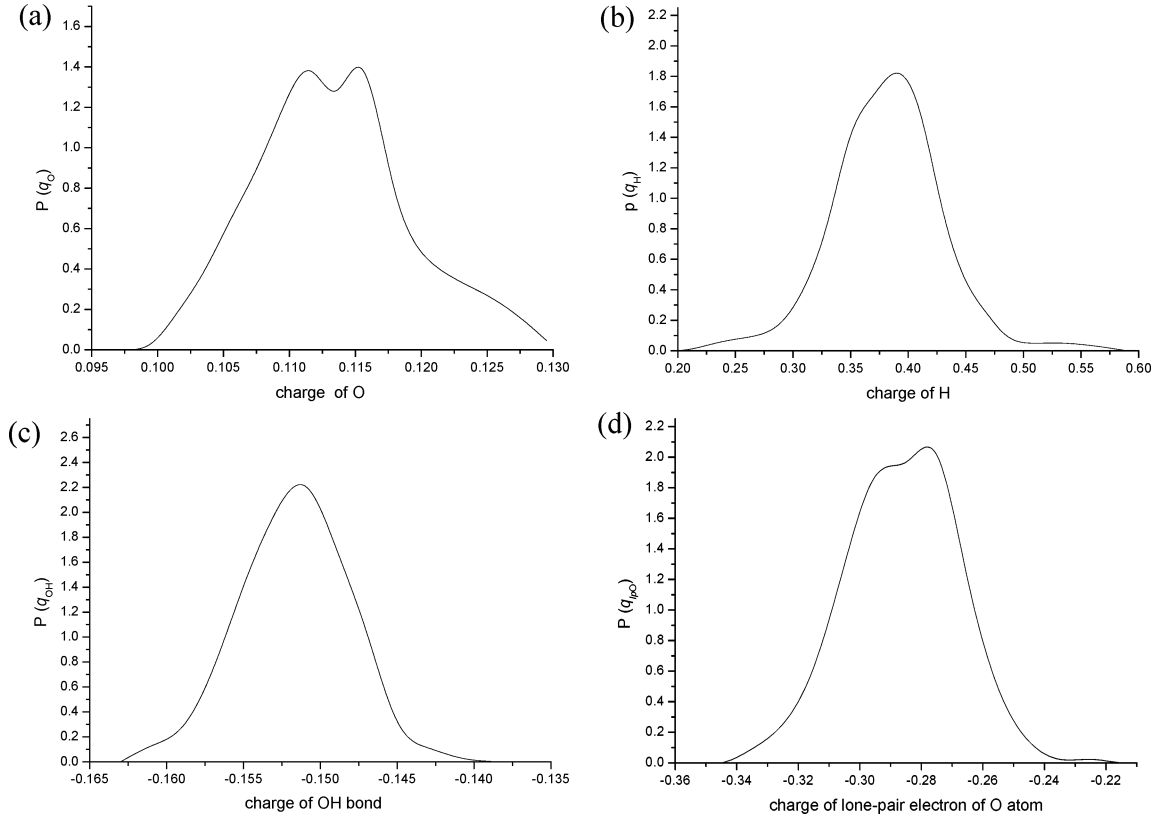

Figure 1. Distribution of charges of (a) O atoms, (b) H atoms, (c) HO bonds, and (d) lone-pair electrons for liquid water at 298 K, as determined by the ABEEM-7P potential.

not accurately reproduce the increase in the bend angle in ice Ih, with respect to the monomer, was due to the linear dipole moment surface (DMS).[84]

4.1.2. Charge Distributions. The charge distributions of atoms, bonds, and lone-pair electrons in the liquid water by the ABEEM-7P water model are shown in Figure 1. Compared to other potentials, the ABEEM-7P model fully considers the conformational changes and molecular vibrations and can give the explicit quantitative charges of all atoms, bonds, and lone-pair electrons. The fixed charge models, such as TIP4P and TIP5P, use fixed charges, which must reflect average or mean field-charge values for the particular phase and have limited transferability to other thermodynamic states; the fluctuating charge TIP4P−FQ model presents the charges based on the EEM also originated from the DFT but uses the TIP4P geometry; the POL5 model, which combines the fluctuating charge and polarizable dipole models, presents the fixed oxygen lone-pair electron charges; and the flexible, polarizable MCDHO model presents the molecular polarizability by a mobile charge, whose position is determined by minimizing the energy for any given atomic configuration. The ABEEM-7P potential gives the positive charges located on O and H atoms, which are balanced by the negative charges located on the O−H bonds and lone-pair electrons. The computed maximum, minimum, and average charge for O atoms via ABEEM-7P in liquid water is ∼0.1006, 0.1309, and 0.1132, respectively; for the H atoms, the corresponding values are 0.2265, 0.5298, and 0.3813, respectively; for the O−H bonds, the corresponding values are −0.1617, −0.1411, and −0.1516, respectively; and, for the lone-pair electrons, the corresponding values are −0.3395, −0.2235, and −0.2862, respectively. Compared to the charges of gas-phase small water clusters $(H_2O)_n$ (n = 1−6), two points must be mentioned:

(1) There are some discrepancies for charges of atoms, bonds, and lone-pair electrons between liquid water and gas-phase small water clusters, because of the different environment around monomer water. For example, the average charge of the O atoms in quasi-cyclic small water clusters $(H_2O)_n$ (n = 2, 3, 4, 5, and 6)[55] is 0.0985, 0.1030, 0.1050, 0.1044, and 0.1050, respectively, and, in the lower energetic conformers[55] of hexamer (cage, book, and prism), the average value is 0.1058, 0.1060, and 0.1062, respectively, whereas, in liquid water, at room temperature, the average charge of the O atoms is 0.1132. Therefore, the more sophisticated charge model is essential to improve a water model that has worked well in all types of environments,[20] especially for some heterogeneous solutions.

(2) Similar to gas-phase small water clusters, it is interesting that, only from charge values, we can observe the bound or free H atoms, and the bound or free lone-pair electrons (the bound H atom means that it takes some contributions to the formation of the hydrogen bond, whereas the free H atom does not). For example, the charges of H atoms in one water molecule are 0.3889 and 0.3885, and it is undoubted that both H atoms must participate in the formation of the hydrogen bond, and then these two H atoms can be called bound H atoms. But the charges of the H atoms in another water molecule are 0.4616 and 0.2913, we can thus obtain such conclusions that one H atom (0.4616) is bound and the other H atom (0.2913) is free. For the bound and free lone-pair electrons, it is same as those of H atoms. The charges of the lone-pair electrons in one water molecule are −0.2881 and −0.2845, which means that both lone-pair electrons are bound, whereas the values of lone-pair electrons in another water molecule are −0.3017 and −0.2607, which means that one (−0.3017) is bound and the other (−0.2607) is free. Figure 1 shows that the charge distributions of the O atoms and lone-pair electrons have two obvious peaks

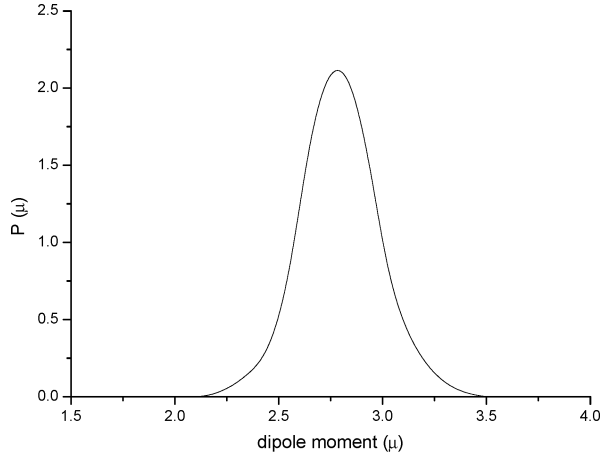

Figure 2. Distribution of the dipole moments of the ABEEM-7P model in liquid water at 298 K.

and the charge distributions of H atoms also has two peaks, although those are not very obvious, which indicates that, at room temperature, there are two different types of lone-pair electrons (or O atoms) and H atoms: one is bound and the other is free. The bound and free atoms or lone-pair electrons are important to further understand the average number of hydrogen bonds per water molecule that is under consideration.

4.1.3. Dipole Moment. Currently, there is some controversy in the literature about the "correct" value of the liquid water dipole moment. A recent analysis of X-ray diffraction (XRD) data by the Soper group, which was the first experimental study of the average dipole moment in liquid water, inferred a value of 2.9 D under ambient conditions.[98] An induction model calculation for the ice Ih lattice gave a dipole moment of 3.09 D.[12] This calculation used more-accurate data as input, as well as higher-order terms in the multipolar expansion than in the 1966 calculation of Coulson and Eisenberg, which gave a value of 2.6 D.[27] DFT calculations on the ice Ih lattice found that the dipole moment can vary with the range of 2.33−2.97 D, depending on how the electronic density was assigned to molecules.[99] Silvestrelli and Parrinello have suggested that the correct value for the liquid-state dipole moment was somewhat larger (∼3.0 D), based on ab initio MD simulations.[100,101] Our ABEEM-7P water model also gives a larger average dipole moment (2.80 D) than those given by some previously reported water models in Table 1 (2.29 D from TIP5P,[20,21] 2.6 D from TIP4P/FQ,[47] and 2.17 D from POL5[58]); however, this value is in good agreement with the latest experimental value (2.9 D) by Soper.[98] In addition, as the electric field that is experienced by the water molecule increases, the flexible body (such as the O−H bond stretching and the H−O−H bond angles decreasing) in value will result in a larger dipole moment, such as the case for the MCDHO model, which predicted a larger dipole moment (3.0 D) than that using ABEEM-7P (2.8 D) and experiment (2.9 D). The distribution of the dipole moment, at room temperature, by ABEEM-7P is shown in Figure 2. ABEEM-7P estimates the dipole moment of water in the range of 2.30−3.39 D, which is broader than the range of 2.4−3.0 D.[54] A broad distribution of dipole moments is observed in both the ab initio and the simulations with polarizable potentials.[12,37,47,50] The full width at half-maximum is fwhm = 0.422 for the ABEEM-7P model, which is similar to the value (fwhm = 0.42) determined by TIP4P-FQ for liquid water at room temperature (298 K).[47] Some papers[54,58,99] have reported that the calculated dipole moment is strongly dependent on the specific method used to partition the continuous charge distribution into molecules. The ABEEM-7P model explicitly partitions the electronic density into atoms, bonds, and lone-pair electrons, and then, as a result, ABEEM-7P may give a reasonable dipole moment that is in fair agreement with the experimental value.[98]

4.1.4. Static Dielectric Constant. The static dielectric constant or permittivity is dependent on the magnitude of the dipole moment, the number of dipoles per unit volume, and the extent to which the directions of the dipoles are correlated. The static dielectric constant (ϵ_0) is calculated from the fluctuations in the total dipole $\boldsymbol{M}$ of the central simulation box, according to[94]

$$\epsilon_0 = \epsilon_\infty + \left(\frac{4\pi\rho}{3kT}\right)\left(\frac{\langle \boldsymbol{M}^2\rangle - \langle \boldsymbol{M}\rangle^2}{N_{\mathrm{mol}}}\right)$$

where ρ is the density, k the Boltzmann's constant, and N_{mol} the total number of molecules. The static dielectric constant provides another estimate of the dipole moment of a water molecule. The computed value by the ABEEM-7P model is shown in Table 1, with the values of TIP5P, TIP4P-FQ, POL5, and the available experimental result. Although the static dielectric constant by the ABEEM-7P potential is slightly small ($\epsilon_0 = 76 \pm 1$), this value is similar to the experimental value ($\epsilon_0 = 78.3$).[102,103] TIP5P and POL5 overestimated this value ($\epsilon_0 = 82 \pm 2$ and 98 ± 8, respectively), and MCDHO did not predict the dielectric constant.

4.1.5. Heat of Vaporization. The heat of vaporization is calculated according to the following formula:[97]

$$\Delta H_{\mathrm{vap}}(T) = -U_{\mathrm{liquid}}(T) + P\Delta V = -U_{\mathrm{liquid}}(T) + RT$$

where ΔH_{vap} is the molar heat of vaporization, U_{liquid} the computed intermolecular potential energy per molecule, P the pressure, and ΔV the molar volume change between liquid and gas. R is the gas constant, and T is the absolute temperature. The computed U_{liquid} and ΔH_{vap} values are given in Table 1, with the corresponding values that were determined by TIP5P,[20] TIP4P-FQ,[47,54] POL5,[58] MCDHO,[45,83] and available experimental values.[100,101] The ABEEM-7P model gives good predictions of U_{liquid} (−10.26 kcal/mol) and ΔH_{vap} (10.85 kcal/mol), in comparison with corresponding experimental values (−9.92 and 10.51 kcal/mol, respectively), and the absolute deviation between ABEEM-7P and experiment is only 0.34 kcal/mol. Two points can be used to explain the slightly larger interaction energy: (i) the parameters of the ABEEM-7P model are fitted not by the interaction energy of liquid water but by the properties of gas-phase water clusters, such as optimal structures, dipole moments, and interaction energies; and (ii) the higher charges and increased anisotropy of the polarizability may result in a slightly attractive intermolecular potential energy, which is similar to other polarizable force fields (such as TIP4P-FQ[54] and MCDHO[45,83]). MCDHO gives larger U_{liquid} and ΔH_{vap} values (−10.40 and 10.99 kcal/mol, respectively) than our ABEEM-7P model and experiment.

4.1.6. Radial Distribution Functions (RDFs). The detailed structure of liquid water is characterized by the radial distribution functions (RDFs). The published RDFs extracted from neutron diffraction or XRD data have varied somewhat over time.[5−7] The experiments of Soper[7] indicated that there was a large experimental uncertainty in the peak heights of the RDFs, perhaps due to the use of different methods for removing the contribution from self scattering or single-atom scattering, whereas the peak position showed much less uncertainty and therefore provided more-reliable points for comparison. The RDFs for the ABEEM-7P model (g_{OO}, g_{OH}, and g_{HH}) and the most recent experiments of the Soper lab[6] at room temperature

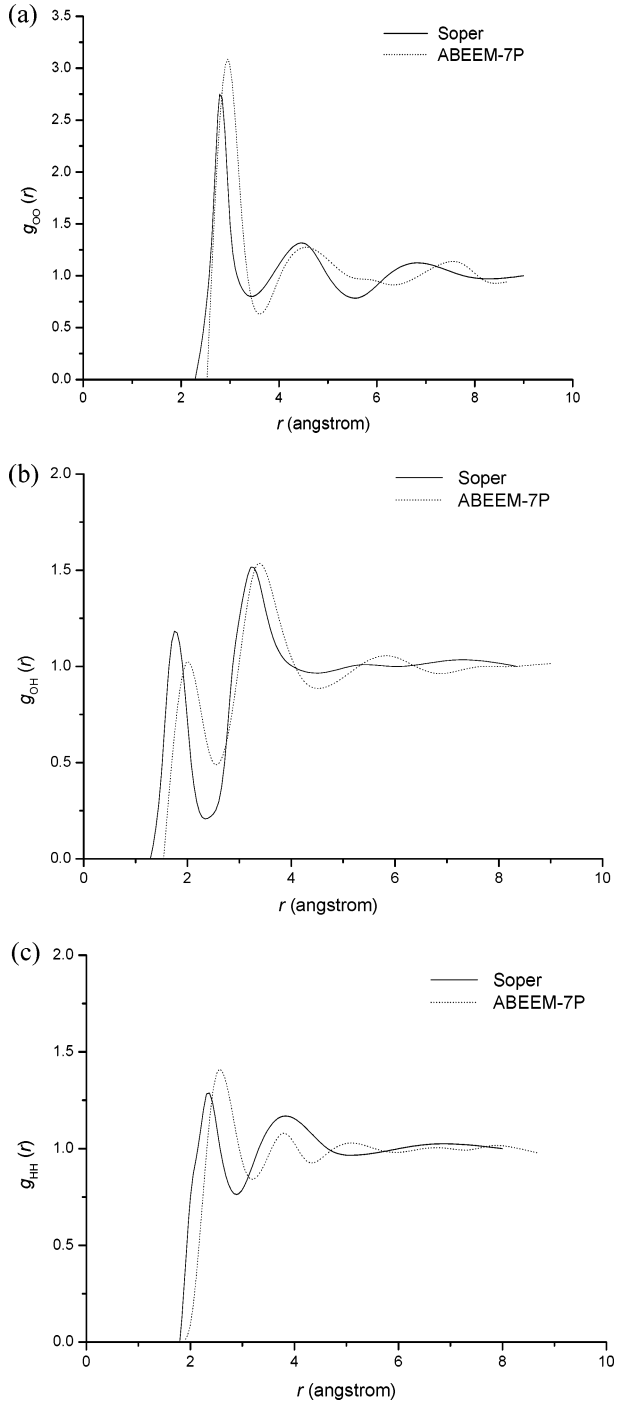

Figure 3. Radial distribution functions (RDFs) at 298 K for the ABEEM-7P potential, compared with the latest results of Soper: (a) oxygen−oxygen RDF, $g_{OO}(r)$; (b) oxygen−hygrogen RDF, $g_{OH}(r)$; and (c) hydrogen−hygrogen RDF, $g_{HH}(r)$.

and pressure are shown in Figure 3. Compared to the fixed-charge model, the fluctuating charge models of g_{OO} have a first peak at a larger distance and present more long-ranged ordering, because of the increased charge.[47] Figure 3a shows that the first peak by ABEEM-7P at ∼3.0 Å, which is slightly larger than the experimental value,[4] corresponds to two hydrogen-bonding water molecules. The first peak of g_{OO} for ABEEM-7P is slightly high and broad, because of the fact that the parameter of ABEEM-7P is based on the structures of gas-phase water clusters; for example, the R_{O-O} of dimmer water by the ABEEM-7P potential is 2.916 Å, which is slightly smaller than the experimental values (2.98 Å), and the values for hexamer isomers are all larger than the available experimental values, to some degree, all of which maybe result in the broader first peak by the ABEEM-7P simulations. However, the average number of H atoms per water molecule by the ABEEM-7P potential is 4.75, which is in reasonable agreement with the experimental value (4.5), and the corresponding value by other empirical force fields is 4.4, 4.5, and 3.9 by TIP4P−FQ, POL5, and TIP5P, respectively. The second peak, which is related to the tetrahedral structure of the nearest neighbors, is located at ∼4.75 Å, which is in reasonable agreement with the experimental value (∼4.50 Å) determined by Soper.

4.1.7. Diffusion Constant. The dynamic properties of water, as determined by the ABEEM-7P model in MD simulations, are also listed in Table 1. The diffusion constant is a very important parameter, because of the fact that it is one of the few time-dependent properties that can be measured directly, both in experiments and in simulations.[23] The diffusion constant D is determined from the Einstein relation:

$$D = \lim_{t\to\infty} \frac{\langle |\boldsymbol{r}_i(t) - \boldsymbol{r}_i(0)|^2 \rangle}{6t}$$

where $\boldsymbol{r}_i(t)$ corresponds to the position vector of the center of mass of molecule i, and the average is taken over all molecules and simulations run in the NVE ensemble. Transport properties are intimately related to the short-range and long-range intermolecular potential.[104] The diffusion constant provides a particularly valuable and fundamental test for a solvent model. Simultaneously, the D is not only related to the fluctuating charge model, which may have a slower diffusion value than the fixed-charge models (primarily because of the stronger electrostatic interactions from the higher charges[47]), but also is related to the internal flexibility, although there is disagreement about whether flexibility increases[77] and decreases[79,80] D. The diffusion constant determined by the flexible and fluctuating-charge ABEEM-7P model ($D = 1.8 \times 10^{-9}$ m^2/s) is smaller than that of the fixed-charge models and is reasonably more similar to the experimental value (2.3×10^{-9} m^2/s).[105] The computed result by the ABEEM-7P water model shows that the internal flexibility decreases D, which is similar to the results of refs 79 and 80.

4.2. Temperature Dependence of Liquid Water Properties. The temperature dependence of the water properties has been examined by many water potentials.[20,23,37,54,97,106,107] Accuracy in the description of water at extreme temperatures is important for liquid water models, because the presence of solutes prevents the solvent from becoming more structural. Most nonpolarizable and polarizable models, such as the commonly used TIP4P, SPC/E and TIP4P-FQ models, do demonstrate the well-known properties of water, including RDFs, the monomer dipole moment, the static dielectric constant, heats of vaporization, etc., under different temperature conditions. The polarizable Bordhole, Sampoli, and Vallauri (BSV)[108] potential designed for the ice Ih phase does not represent the properties of liquid water well; thus, apparently, no single potential has been shown to reproduce the properties of both the liquid and ice phases accurately. Recently, the TIP4P-FQ model[54] introduced by Rick has been used to compute the dipole moment in three phases: liquid, gas, and ice Ih. However, the static dielectric constants at the lower temperature were not very good. Rick et al. indicated that the confidence in the predictions of solvent structure around solutes would therefore be increased if the potential has been demonstrated to be a good model for different temperature conditions. Moreover, until now, no polarizable

TABLE 2: Average, Minimum, and Maximum Charges of O Atoms, H Atoms, O−H Bonds, and Lone-Pair Electrons, as Determined by ABEEM-7P under Different Temperatures

	Charge		
temperature (K)	average	minimum	maximum
	O Atom		
260	0.1130	0.0983	0.1284
273	0.1133	0.0989	0.1295
298	0.1132	0.1006	0.1319
310	0.1130	0.0974	0.1318
348	0.1121	0.0958	0.1317
	H Atom		
260	0.3812	0.2253	0.5602
273	0.3815	0.2529	0.5224
298	0.3813	0.2265	0.5298
310	0.3798	0.2214	0.5082
348	0.3730	0.2411	0.5063
	OH Bond		
260	−0.1516	−0.1638	−0.1375
273	−0.1518	−0.1638	−0.1414
298	−0.1516	−0.1617	−0.1383
310	−0.1516	−0.1622	−0.1383
348	−0.1512	−0.1623	−0.1402
	Lone-Pair Electron		
260	−0.2861	−0.3386	−0.2252
273	−0.2864	−0.3325	−0.2282
298	−0.2862	−0.3395	−0.2235
310	−0.2847	−0.3284	−0.2146
348	−0.2776	−0.3311	−0.2192

water models could give the explicit charges of a water molecule, which is important, because of the fact that the dipole moment and static dielectric constant are dependent on how the electric density is assigned to molecules.[99] In addition, Mahoney and Jorgensen[20] showed that further improvement in the computed results, e.g., at high temperature and pressure, would likely necessitate the use of a larger number of charged sites or explicit polarization, as well as much effort in regard to optimization of the model. An important aim of our macromolecular simulations is to investigate how water properties are affected by non-native conditions, such as extreme temperatures. It is significant to demonstrate that the water model itself reproduces the experimentally observed dependence of water properties on temperature, and it is also important to develop a water model to describe the properties of a biological solute.

4.2.1. Charge Distribution. The charges of O atoms, H atoms, O−H bonds, and lone-pair electrons for liquid water over a temperature range of 260−348 K are calculated by the ABEEM-7P potential, and Table 2 lists the average, minimum, and maximum charges of O atoms, H atoms, O−H bonds, and lone-pair electrons. Figure 4 presents the charge distributions of O atoms, H atoms, O−H bonds, and lone-pair electrons, respectively, under the different temperature conditions. The similarities for charges between 298 K and other temperatures are as follows. One is that, at all temperatures, the positive charges by ABEEM-7P are located on O and H atoms, which are balanced by the negative charges located on the O−H bonds and lone-pair electrons. In addition, from the charges of O atoms, H atoms, O−H bonds, and lone-pair electrons, we can determine the bound H atoms and lone-pair electrons that participate in the formation of a hydrogen bond and the free H atoms and lone-pair electrons that do not participate in the formation of a hydrogen bond. For example, compared to the charges of gas-phase water clusters $(H_2O)_n$ ($n = 1-6$),[55] at 260 K, the H atom charges of one water molecule are 0.3849 and 0.3963, and it is easy to observe that both H atoms are bound; at 273 K, the H atom charges of one water molecule are 0.4685 and 0.2716, and it is undoubted that one (0.4685) is bound and the other (0.2716) is free. Similar to that observed for H atoms, at 310 K, the lone-pair electrons of the O atom of one water molecule are −0.2823 and −0.2893, both of which are bound, and at 348 K, the lone-pair electrons of the O atom are −0.2901 and −0.2564; then, one (−0.2901) is bound and the other (−0.2564) is free. The bound H atoms and lone-pair electrons, and the free H atoms and lone-pair electrons, are useful to understand the temperature dependence of the water structure and the average number of hydrogen bonds per water molecule over a range of temperature. From the comparison of charges of O atoms, H atoms, O−H bonds, and lone-pair electrons under different temperature by the ABEEM-7P potential, two distinctions can be observed:

(1) Under different temperatures, the average charges of O atoms, H atoms, O−H bonds, and lone-pair electrons (listed in Table 2) are different, although the differences are not very large. For example, the average charge of the O atoms is 0.1130, 0.1133, 0.1132, 0.1130, and 0.1121, respectively, for temperatures of 260, 273, 298, 310, and 348 K, among which the O atom charge at 348 K (0.1121) is minimal and most similar to the charge of the gas-phase monomer water (0.1125).[55] Such results are reasonable because, as the temperature increases, the density decreases while the volume increases; then, the long-range interactional effect between different water molecules will be small and the magnitude of the absolute charge will be somewhat smaller at high temperature than that at low temperature. The average charges of H atoms, O−H bonds, and lone-pair electrons can be observed to have similar results, with the values of the O atom, and, at 348 K, the absolute average charge of H atom, O−H bonds, and a lone-pair electron is 0.3730, 0.1512, and 0.2776, respectively.

(2) The charge distributions of the O atoms (Figure 4a) and H atoms (Figure 4b) show that the two small peaks are very obvious at lower temperature, and as the temperature increases, such two peaks are becoming indistinct, only from which we can find some structural information of liquid water that the arrangement of water molecules at the lower temperature is more

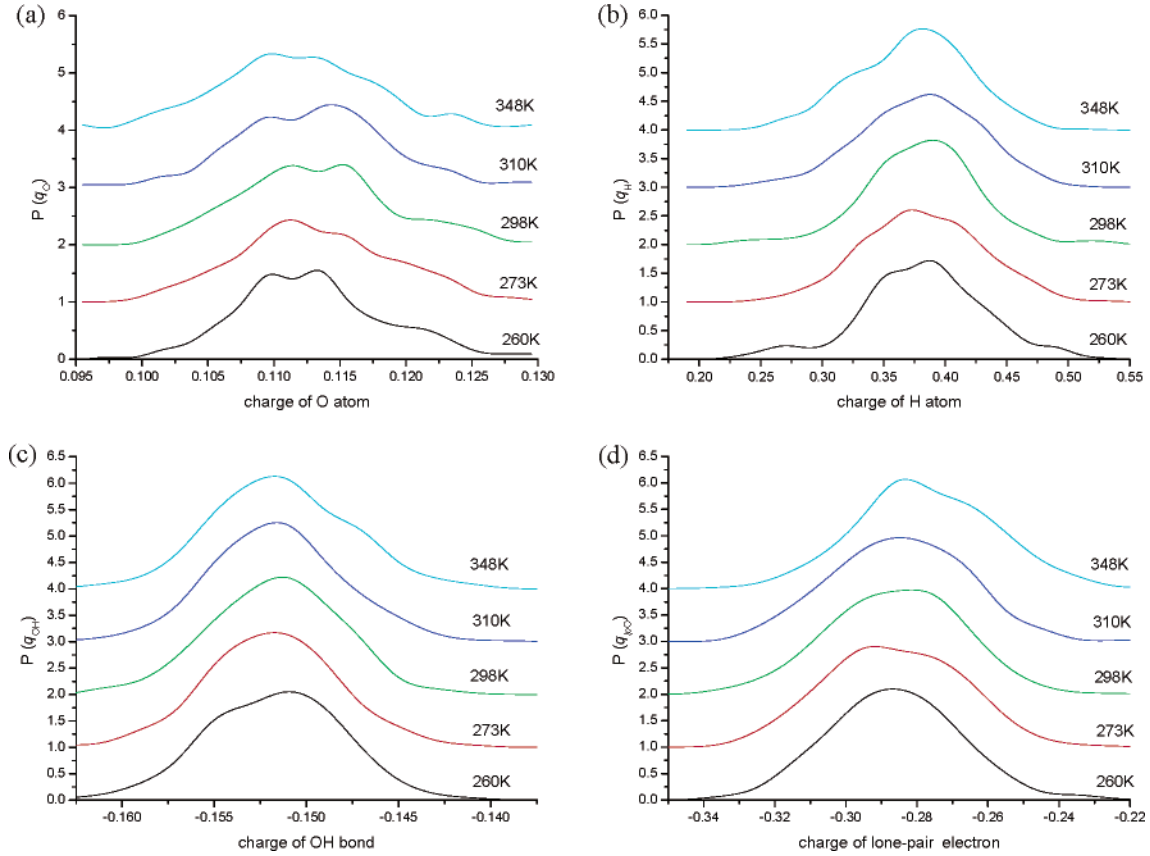

Figure 4. Temperature dependence of charge distribution of (a) O atoms, (b) H atoms, (c) HO bonds, and (d) lone-pair electrons for liquid water, as determined by the ABEEM-7P potential.

ordered than that at the higher temperature. Overall, the charges of water system are different under different ambient conditions (i.e., the different temperature), and the ABEEM-7P water model can consider the clear charges of O atoms, H atoms, O−H bonds, and lone-pair electrons, especially for short-range interaction of the hydrogen bonds over a range of temperature. It seems explicit at this point that the addition of charged sites and the explicit description of charges will lead to an improved water model.

4.2.2. Dipole Moment and Static Dielectric Constant. The average dipole moments by the ABEEM-7P water model for liquid water under different temperatures are given in Table 3, with available results by TIP4P-FQ[54] and TIP5P.[20] For the water liquid, the dipole moment determined by the ABEEM-7P potential steadily decreases as a function of temperature, which is consistent with the TIP4P-FQ values, although the magnitude of the values of the former is slightly larger than that of the latter. For example, at 260 K, the average dipole moment of ABEEM-7P is 2.832 D, whereas that of TIP4P-FQ is 2.805 D; at 310 K, the average dipole moment of ABEEM-7P is 2.762 D, whereas that of TIP4P-FQ is 2.606 D. With increasing temperature, the difference between the ABEEM-7P and TIP4P-FQ models is changed (becomes larger); i.e., the range of the average dipole moment from 260 K to 310 K for the ABEEM-7P model (0.05) is smaller than that for the TIP4P-FQ model (0.2). The distributions of the dipole moment of ABEEM-7P under the different temperatures are depicted in Figure 5. As the temperature increases, the distribution becomes narrower; the fwhm value is 0.489 for 260 K, 0.470 for 273 K, 0.422 for 298 K, 0.404 for 310 K, and 0.350 for 348 K. The ABEEM-7P distribution of the dipole moment at high temperature is more narrow and the average dipole moment becomes larger with decreasing temperature, indicating that the liquid water by the ABEEM-7P potential at low temperature is a more polarizable environment, which is consistent with other estimates.[54]

Results for the dielectric constant of the ABEEM-7P water model over the temperature range of 260−348 K at 1 atm pressure are presented in Table 3 and Figure 6. Also plotted in the figure are the experimental values[102,103,109] and results by other potentials.[20,37,43] Although the ABEEM-7P model slightly underestimates the dielectric constant, it gives a good estimate over a range of temperature selected. Especially at the high temperature (348 K), our calculated value of 63 is very similar to the experimental value (62.59). Although the TIP4P-FQ and TIP5P models also give good values for the dielectric constant over a range of temperature, TIP4P-FQ and TIP5P may overestimate the temperature dependence, compared to the ABEEM-7P model. It has also suggested that a better description of the fluctuating charge and a more-complicated description of charged sites are important factors for improved reproduction of the dielectric constant.[20]

4.2.3. Heats of Vaporization. Table 3 also presents the liquid-state energy and heats of vaporization for ABEEM-7P, as a function of temperature, and the corresponding values are plotted in Figure 7 with the results of TIP5P,[20] TIP4P-FQ,[54] and experiments.[110] The experimental heats of vaporization are well-reproduced by ABEEM-7P over a range of temperatures. Using the ABEEM-7P potential, the heats of vaporization are 11.40, 11.13, 10.85, 10.64, and 9.84 kcal/mol at 260, 273, 298, 310, and 348 K, respectively, whereas the respective experimental values are 10.90, 10.76, 10.51, 10.39, and 9.69 kcal/mol. Compared to that of experiments, heats of vaporization obtained using ABEEM-7P are slightly larger than the experimental values at all calculated temperatures; however, with the increas-

TABLE 3: Temperature Dependence of Liquid Properties Determined Using the ABEEM-7P Model, Including Energy (U_{liquid}), Heat of Vaporization (ΔH_{vap}), Average Dipole Moment (μ), and Static Dielectric Constant (ϵ_0)[a]

temperature (K)	Value			
	ABEEM-7P	TIP4P-FQ[b]	TIP5P[c]	expt[d]
		U_{liquid} (kcal/mol)		
260	−10.88 ± 0.04	−11.08 ± 0.03	−10.85 ± 0.01	−10.38
273	−10.59 ± 0.09	−10.61 ± 0.02	−10.50 ± 0.01	−10.22
298	−10.26 ± 0.08	−9.89 ± 0.02	−9.87 ± 0.01	−9.92
310	−10.02 ± 0.09	−9.63 ± 0.01	−9.59 ± 0.01	−9.77
348	−9.15 ± 0.28		−8.83 ± 0.01	−9.00
		ΔH_{vap} (kcal/mol)		
260	11.40 ± 0.04	11.60 ± 0.03	11.37 ± 0.01	10.90
273	11.13 ± 0.09	11.15 ± 0.02	11.04 ± 0.01	10.76
298	10.85 ± 0.08	10.48 ± 0.02	10.46 ± 0.01	10.51
310	10.64 ± 0.09	10.25 ± 0.01	10.21 ± 0.01	10.39
348	9.84 ± 0.28		9.52 ± 0.01	9.69
		μ (D)		
260	2.83 ± 0.01	2.805 ± 0.005		
273	2.82 ± 0.01	2.733 ± 0.004		
298	2.80 ± 0.01	2.641 ± 0.001	2.29	
310	2.78 ± 0.01	2.606 ± 0.002		
348	2.74 ± 0.01			
		ϵ_0		
260	92 ± 2	105 ± 27		
273	83 ± 1	97 ± 19	91.8 ± 1.5	87.9
298	76 ± 1	79 ± 8	81.5 ± 1.6	78.4
310	73 ± 2	78 ± 2		74.2
348	63 ± 1			62.6

[a] Also shown are the experimental values, which, for some temperatures, are interpolations between the reported data points. [b] Data taken from ref 54. [c] Data taken from refs 20 and 21. [d] Experimental data for U_{liquid}, ΔH_{vap}, and μ taken from ref 110; experimental data for ϵ_0 taken from refs 102 and 103.

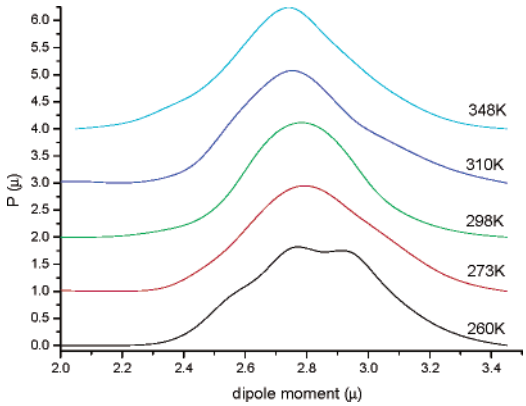

Figure 5. Temperature dependence of the dipole moment distribution of liquid water, as determined by the ABEEM-7P potential.

ing temperature, the difference becomes small (the difference at 348 K between ABEEM-7P and experiment is only 0.15 kcal/mol). Comparison with the ABEEM-7P water model shows that the TIP4P-FQ and TIP5P potentials also reproduce the experimental energy over a range of temperature; however, the value is slightly too large at low temperatures and too low at high temperatures, especially for the TIP4P-FQ model, for example, at 260 K, the heat of vaporization by TIP4P-FQ is 11.60 kcal/mol, and at 310 K, the value is 10.25 kcal/mol, which is largely dependent on the temperature.

4.2.4. Radial Distribution Function. The water structure is also affected by increasing temperature, and the temperature dependence of the RDFs determined by the ABEEM-7P model is illustrated in Figure 8. The expected reduction in structure

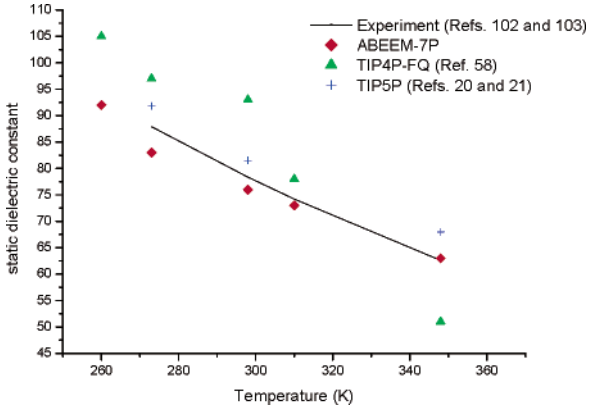

Figure 6. Temperature dependence of the static dielectric constant (ϵ_0). The ABEEM-7P, TIP4P-FQ, and TIP5P water potentials all reproduce the trend of experimental ϵ_0 over a range of temperatures. The results of the TIP4P-FQ model are too large in magnitude at low temperatures and too low in magnitude at high temperatures, and TIP5P overestimates ϵ_0 at all temperature points. The ABEEM-7P model agrees well with the experimental values over a range of temperature, especially at high temperature, which indicates that a better description of the charge of the hydrogen bonds and a more complicated description of the charged sites are important factors for improved reproduction of ϵ_0.

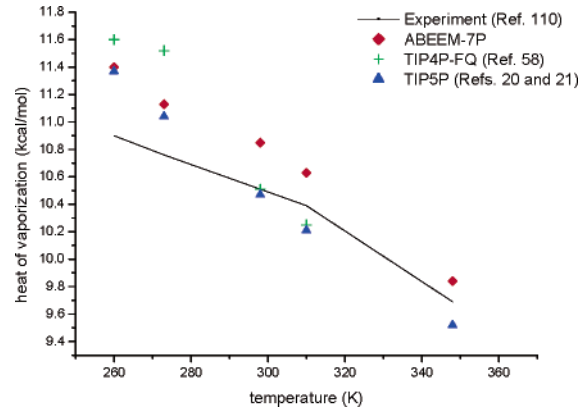

Figure 7. Temperature dependence of heats of vaporization (ΔH_{vap}). The results of TIP4P-FQ and TIP5P are all slightly too large at low temperatures and too low at high temperatures. The ABEEM-7P model also obtains the trend of the temperature dependence of ΔH_{vap}, in reasonable agreement with the experimental values, although over the range of temperatures, the ΔH_{vap} value of ABEEM-7P is larger than that of the experiments, because the energy is too attractive. However, the discrepancy of ΔH_{vap} between ABEEM-7P and the experiment is becoming smaller with increasing temperature.

with increasing temperature is observed, to some degree. The separation of nearest and second-nearest neighbors becomes slight sharper in the oxygen−oxygen RDF (g_{OO}) at 260 K, which is consistent with adoption of a more ice-I-like structure. Also, in the g_{OO} RDF, as the temperature increases, the first valley and second peak quickly approach a value of 1, which is indicative of no structure. Although the height of the first peak of g_{OO} decreases, the decline is not very large, indicating that there is a significant first-neighbor structure, even at the high temperature. Thus, at high temperature, the short-range structure due to direct hydrogen-bonding interactions is maintained, whereas the longer-range structure is lost, which has been explicitly shown by the temperature dependence of charges of O atoms, H atoms, O−H bonds, and lone-pair electrons computed by the ABEEM-7P potential and also agrees with the previous results reported by other potentials.

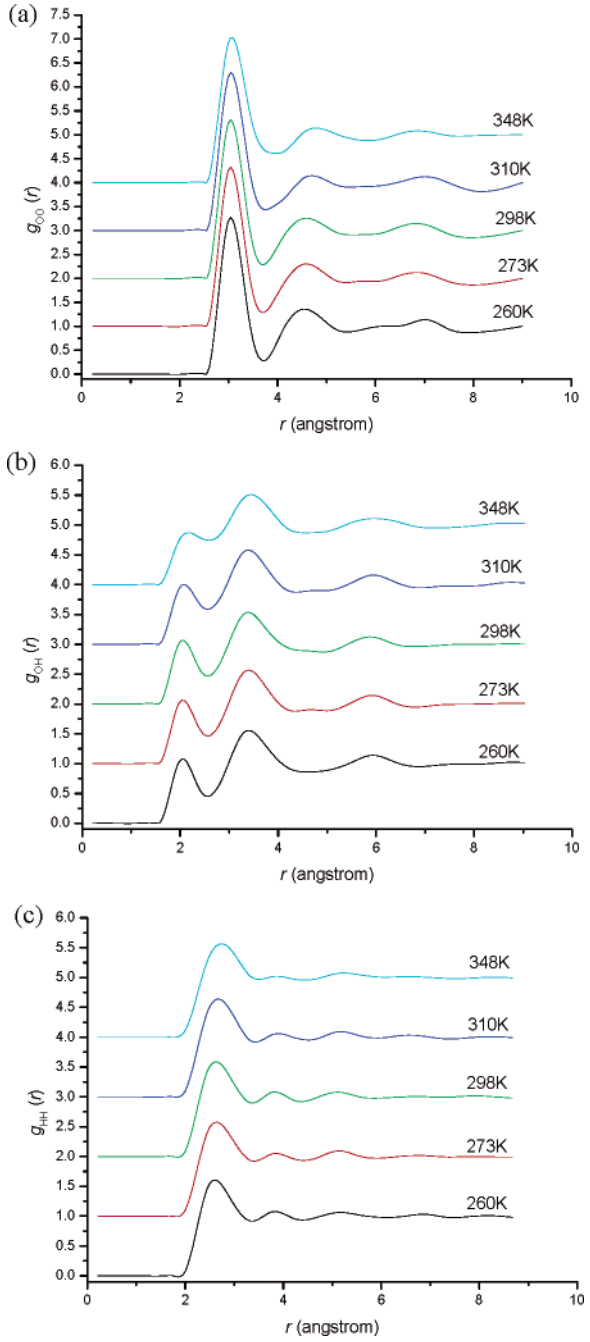

Figure 8. Variation of the RDF as a function of temperature: (a) oxygen−oxygen, $g_{OO}(r)$; (b) oxygen−hydrogen, $g_{OH}(r)$; and (c) hydrogen−hydrogen, $g_{HH}(r)$. For $g_{OO}(r)$, the height of the first peak is a slow function of temperature, whereas the depth of the first valley and the height of the second peak are affected much more.

5. Conclusion

We have studied the structural and dynamic properties of liquid water over a range of temperatures using a transferable, intermolecular potential, seven-points approach, including fluctuating charges and flexible body model (ABEEM-7P) based on an atom-bond electronegativity equalization method (ABEEM) fused into molecular mechanics (MM). At room temperature, the average ABEEM-7P bond length (0.968 Å) in the liquid phase is shifted toward longer length, which is in excellent agreement with recent experimental measurements (0.970 Å). Meanwhile, the ABEEM-7P simulations show a H−O−H angle (102.8°) that is consistent with an earlier reported experimental angle (102.8°) and values obtained by other flexible body water models, such as MCDHO in the liquid phase (102.79°) but contrary to a slightly larger angle that was deduced from recent experimental measurements (106°). The ABEEM-7P model applies the ABEEM model to explicitly compute the charges of O atoms, H atoms, O−H bonds, and lone-pair electrons for every monomer in the liquid. Especially, by introducing a specific expression $k_{lp,h}(R_{lp,H})$, the ABEEM-7P model explicitly explores the electrostatic interaction of the hydrogen-bond network in the liquid water. From the quantitative charges of O atoms, H atoms, O−H bonds, and lone-pair electrons, we can easily observe the bound and free H atoms, and bound and free lone-pair electrons of the O atoms, which are important to understand the structure of hydrogen bond network further at different temperatures. At room temperature, the ABEEM-7P force field gives satisfactory predictions for the properties of liquid water, in comparison to experiments. The dipole moment (μ = 2.80 D), static dielectric constant (ϵ_0 = 76), and heat of vaporization (ΔH_{vap} = 10.85 kcal/mol) by ABEEM-7P are in reasonable agreement with the available experimental values (2.9 D, 78.3, and 10.51 kcal/mol, respectively). In addition, although the peaks of liquid-state radial distribution functions (RDFs) by ABEEM-7P are slightly deviated, in comparison with the experimental measurements, the average number of H atoms per water molecule is 4.75 which is similar to the experimental value (4.5). The diffusion constants computed by the polarizable models, such as ABEEM-7P (1.8×10^{-9} m^2/s), POL5 (1.81×10^{-9} m^2/s), and TIP4P-FQ (1.9×10^{-9} m^2/s), are all smaller than the value determined by the experiment (2.3×10^{-9} m^2/s).

The ABEEM-7P model also gives satisfactory results under ambient conditions and performs well for the temperature dependence (260−348 K) of liquid-phase properties. The quantitative charges of O atoms, H atoms, O−H bonds, and lone-pair electrons from 260 K to 348 K are explicitly computed by the ABEEM-7P potential. The absolute average charges of O atoms, H atoms, O−H bonds, and lone-pair electrons are minimal at the computed higher temperature (348 K), and the two peaks of O and H atom charge distribution have a tendency to be indistinct with increasing temperature. In addition, the width of the dipole moment distribution slightly decreases as the temperature increases. The static dielectric constant and heats of vaporization, as a function of temperature, are reproduced and agree reasonably well with the experimental values from 260 K to 348 K; the deviations at 260−298 K are somewhat large, whereas the computed values by the ABEEM-7P potential are very similar to the experimental values at 310 and 348 K. The expected reduction in structure from the RDF with increasing temperature is observed, which is consistent with experimental and other water potential results.

Overall, the ABEEM-7P model shows some improvements for the liquid water over previous water models. The combination of atom-bond electronegativity equalization method and molecular mechanics (ABEEM/MM), not only including the vibration of bond length and angle, but also including explicit consideration of electrostatic interaction of atoms, bonds, and lone-pair electrons (especially, the short-range interaction of hydrogen bond), shows that it can reproduce rather accurate properties of liquid water over a range of temperature. It would be interesting to (i) extend this work by comparing the density at different temperatures (they are not computed in the present study because of the slower convergence by a flexible and fluctuating charge model) and (ii) simulate biochemical systems in liquid water; both possibilities are currently being considered.

Acknowledgment. The authors greatly thank Professor Jay William Ponder for providing the Tinker program. We also thank the comments of the editor and reviewers. This work is supported by a grant from the National Science Foundation of China (No. 20373021).

References and Notes

(1) Roentgen, W. C. *Annu. Rev. Phys. Chem.* **1892**, *45*, 91.
(2) Bernal, J. D.; Fowler, R. H. *J. Chem. Phys.* **1933**, *1*, 515.
(3) Narten, A. H.; Levy, H. A. *J. Chem. Phys.* **1971**, *55*, 2263.
(4) Soper, A. K.; Philips, M. G. *Chem. Phys*. **1986**, *107*, 47.
(5) Soper, A. K.; Turner, J. *Int. J. Mod. Phys. B* **1993**, *7*, 3049.
(6) Soper, A. K.; Bruni, F.; Ricci, M. A. *J. Chem. Phys.* **1997**, *106*, 247.
(7) Soper, A. K. *Chem. Phys*. **2000**, *258*, 121.
(8) Postorine, P.; Tromp, R. H.; Riui, M.-A.; Soper, A. K.; Neilson, W. *Nature* **1993**, *366*, 668.
(9) Mills, R. *J. Phys. Chem*. **1973**, *77*, 685.
(10) Price, W. S.; Ide, H.; Arata, Y. *J. Phys. Chem. A* **1999**, *103*, 448.
(11) Laasonen K.; Sprik, M.; Parrinello, M.; Car, R. *J. Chem. Phys*. **1993**, *99*, 9080.
(12) Silvestrelli, P. L.; Parrinello, M. *J. Chem. Phys.* **1999**, *111*, 3572.
(13) Dell Site, L.; Alavi, A.; Lynden-Bell, R. M. *Mol. Phys.* **1999**, *96*, 1683.
(14) Stillinger, F. H.; Rahman, A. *J. Chem. Phys*. **1974**, *60*, 1545.
(15) Berendsen, H. J. C.; Postma, J. P. M.; van Gunsteren, W. F.; Hermans, J. Interaction Models for Water in Relation to Protein Hydration. In *Intermolecular Forces*; Pullman, B., Ed.; Reidel: Dordrecht, The Netherlands, 1981.
(16) Jorgensen, W. L.; Chandrasekhar, J.; Madura, J. D.; Impey, R. W.; Klein, M. L. *J. Chem. Phys.* **1983**, *79*, 926.
(17) Berendsen, H. J. C.; Grigera, J. R.; Straatsma, T. P. *J. Phys. Chem.* **1987**, *91*, 6269.
(18) Dang, L. X.; Pettitt, B. M. *J. Phys. Chem*. **1987**, *91*, 3349.
(19) Jorgensen, W. L. *J. Am. Chem. Soc*. **1981**, *103*, 335.
(20) Mahoney, M. W.; Jorgensen, W. J. *J. Chem. Phys.* **2000**, *112*, 8910.
(21) Mahoney, M. W.; Jorgensen, W. L. *J. Chem. Phys.* **2001**, *114*, 363.
(22) Glättli, A.; Daura, X.; van Gunsteren, W. F. *J. Chem. Phys.* **2002**, *116*, 9811.
(23) Levitt, M.; Hirshberg, M.; Sheron, R.; Laidig, K. E.; Daggett, V. *J. Phys. Chem. B* **1997**, *101*, 5051.
(24) Mark, P.; Nilsson, L. Structure and Dynamics of the TIP3P, SPC, and SPC/E Water Models at 298 K. *J. Phys. Chem. A* **2001**, *105* (43), 9954.
(25) Glättli, A.; Daura, X.; van Gunsteren, W. F. *J. Comput. Chem*. **2003**, *24*, 1087.
(26) Gregory, J. K.; Clary, D. C.; Liu, K.; Brown, M. G.; Saykally, R. J. *Science* **1997**, *275*, 814.
(27) Coulson, C. A.; Eisenberg, D. *Proc. R. Soc. London, Ser. A* **1966**, *291*, 445.
(28) Sorenson, J. M.; Hura, G.; Glaeser, R. M.; Head-Gordon, T. *J. Chem. Phys*. **2000**, *113*, 9149.
(29) Silvestrelli, P. L.; Parrinello, M. *Phys. Rev. Lett.* **1999**, *82*, 3348.
(30) Batista, E. R.; Xantheas, S. S.; Jónsson, H. *J. Chem. Phys.* **1998**, *109*, 4546.
(31) Stillinger, F. H.; David, C. W. *J. Chem. Phys.* **1978**, *69*, 1473.
(32) Barnes, P.; Finney, J. L.; Nicholas, N. D.; Quinn, J. E. *Nature* **1979**, *282*, 459.
(33) Rullman, J. A. C.; van Duijnen, P. T. *Mol. Phys*. **1998**, *63*, 451.
(34) Sprik, M.; Klein, M. L. *J. Chem. Phys*. **1988**, *89*, 7556.
(35) Ahlström. P.; Wallqvist, A.; Engström, S.; Jönsson, B. *Mol. Phys*. **1989**, *68*, 563.
(36) Cieplak, P.; Kollman, P.; Lybrand, J. *J. Chem. Phys*. **1990**, *92*, 6755.
(37) Svishchev, I. M.; Kusalik, P. G.; Wang, J.; Boyd, R. J. *J. Chem. Phys.* **1996**, *105*, 4742.
(38) Dang, L. X. *J. Chem. Phys*. **1992**, *87*, 2659.
(39) Wallqvist, A.; Berne, B. J. *J. Phys. Chem*. **1993**, *97*, 13841.
(40) Bernardo, D. N.; Ding, Y. B.; Kroghjespersen, K.; Levy, R. M. *J. Phys. Chem.* **1994**, *98*, 4180.
(41) Caldwell, J. W.; Kollman, P. A. *J. Phys. Chem*. **1995**, *99*, 6208.
(42) Chialvo, A. A.; Cummings, P. T. *J. Chem. Phys.* **1996**, *105*, 8274.
(43) Chen, B.; Xing, J. H.; Siepmann, J. I. *J. Phys. Chem. B* **2000**, *104*, 2391.
(44) Halgren, T. A.; Damm, W. *Curr. Opin. Struct. Biol*. **2001**, *11*, 236.
(45) Stern, H. A.; Berne, B. J. *J. Chem. Phys*. **2001**, *115*, 7622.
(46) Zhu, S. B.; Singh, S.; Robinson, G. W. *J. Chem. Phys*. **1991**, *95*, 2791.
(47) Rick. S. W.; Stuart, S. J.; Berne, B. J. *J. Chem. Phys*. **1994**, *101*, 6146.
(48) Rick, S. W.; Berne, B. J. *J. Am. Chem. Soc*. **1996**, *118*, 672.
(49) Perng, B.−C.; Newton, M. D.; Raineri, F. O.; Friedman, H. L. *J. Chem. Phys*. **1996**, *104*, 7153.
(50) Field, M. *J. Mol. Phys.* **1997**, *91*, 835.
(51) Liu, Y. P.; Kim, K.; Berne, B. J.; Friesner, R. A.; Rick, S. W. *J. Chem. Phys.* **1998**, *108*, 4739.
(52) Banks, J. L.; Kaminski, G. A.; Zhou, R.; Maina, D. T.; Berne, B. J.; Friesner, R. A. *J. Chem. Phys.* **1999**, *110*, 741.
(53) Rick. S. W.; Cachau, R. E. *J. Chem. Phys.* **2000**, *112*, 5230.
(54) Rick, S. W. *J. Chem. Phys*. **2001**, *114*, 2276.
(55) Yang, Z. Z.; Wu, Y.; Zhao, D. X. *J. Chem. Phys*. **2004**, *120*, 2541.
(56) Soetens, J.-C.; Millot, C. *Chem. Phys. Lett.* **1995**, *235*, 22.
(57) Stern, H. A.; Kaminski, G. A.; Banks, J. L.; Zhou, R.; Berne, B. J.; Friesner, R. A. *J. Phys. Chem. B* **1999**, *103*, 4730.
(58) Stern, H. A.; Rittner, F.; Berne, B. J.; Friesner, R. A. *J. Chem. Phys*. **2001**, *115*, 2237.
(59) Nalewajski, R. F. *J. Am. Chem. Soc.* **1984**, *106*, 944.
(60) Mortier, W. J.; Ghosh, S. K.; Shankar, S. *J. Am. Chem. Soc*. **1986**, *108*, 4315.
(61) Baekelandt, B. G.; Mortier, W. J.; Lievens, J. L.; Schoonheydt, R. A. *J. Am. Chem. Soc*. **1991**, *113*, 6730.
(62) Baekelandt, B. G.; Mortier, W. J.; Schoonheydt, R. A. *Struct. Bonding (Berlin)* **1993**, *80*, 187.
(63) Baekelandt, B. G.; Jassens, G. O. A.; Toufar, H.; Mortier, W. J.; Schoonheydt, R. A. *J. Phys. Chem*. **1995**, *99*, 9784.
(64) Janssens, G. O. A.; Toufar, H.; Baekelandt, B. G.; Mortier, W. J.; Schoonheydt, R. A. *Stud. Surf. Sci. Catal.* **1997**, *105*, 725.
(65) Yang, Z. Z.; Wang, C. S. *J. Phys. Chem. A* **1997**, *101*, 6315.
(66) Wang. C. S.; Li. S. M.; Yang, Z. Z. *J. Mol. Struct. (THEOCHEM)* **1998**, *430*, 191.
(67) Wang, C. S.; Yang, Z. Z. *J. Chem. Phys*. **1999**, *110*, 6189.
(68) Cong, Y.; Yang, Z. Z. *Chem. Phys. Lett*. **2000**, *316*, 324.
(69) Yang, Z. Z.; Wang, C. S. *J. Theor. Comput. Chem*. **2003**, *2*, 273.
(70) Parr, R. G.; Yang, W. *Density Functional Theory of Atom and Molecules*; Oxford University Press: New York, 1989.
(71) Parr, R. G.; Donnelly, R. A.; Levy, R. A.; Palke, W. E. *J. Chem. Phys*. **1978**, *68*, 3801.
(72) Donnelly, R. A.; Parr, R. G. *J. Chem. Phys*. **1978**, *69*, 4431.
(73) Sanderson, R. T. *Chemical Bond and Bond Energies*; Academic Press: New York, 1976.
(74) Sanderson, R. T. *Polar Covalence*; Academic Press: New York, 1983.
(75) Stillinger, F. H.; Rahman, A. *J. Chem. Phys.* **1978**, *68*, 666.
(76) Toukan, K.; Rahman, A. *Phys. Rev. B.: Condens. Matter* **1985**, *31*, 2643.
(77) Teleman, O.; Ahlström, P. *J. Am. Chem. Soc.* **1986**, *108*, 4333.
(78) Reimers, J. R.; Watts, R. O. *Chem. Phys.* **1984**, *91*, 201.
(79) Barrat, J.-L.; McDonald, I. R. *Mol. Phys.* **1990,** *20*, 535.
(80) Anderson, J.; Ullo, J.; Yip, S. *J. Chem. Phys.* **1987**, *87*, 1726.
(81) Wallqvist, A.; Berne, B. J. *Chem. Phys. Lett.* **1985**, *117*, 214.
(82) Zhu, S. B.; Yao, S.; Zhu, J. B.; Singh, S.; Robinson, G. W. *J. Phys. Chem.* **1991**, *95*, 6211.
(83) Saint-Martin, H.; Henández-Cobos, J.; Bernal-Uruchurtu, M. I.; Ortega-Blake, I.; Berendsen, H. J. C. *J. Chem. Phys*. **2000**, *13*, 10899.
(84) Burnham, C. J.; Xantheas, S. S. *J. Chem. Phys*. **2002**, *116*, 5115.
(85) Ichikawa, K.; Kameda, Y.; Yamaguchi, T.; Wakita, H.; Misawa, M. *Mol. Phys.* **1991**, *73*, 79.
(86) Thiessen, W. E.; Narten, A. M. *J. Chem. Phys*. **1982**, *77*, 2656.
(87) Speedy, R. J.; Madura, J. D.; Jorgensen, W. L. *J. Phys. Chem*. **1987**, *91*, 909.
(88) Liu, K.; Brown, M. G.; Carter, C.; Saykally, R. J.; Gregory, J. K.; Clary, D. C. *Nature* **1996**, *381*, 501.
(89) Yang, Z. Z.; Zhao, D. X. *Chem. Phys. Lett*. **1998**, *292*, 387.
(90) Berendsen, H. J. C.; van der Spoel, D.; van Drumen, R. *Comput. Phys. Commun.* **1995**, *91*, 43.
(91) Kell, G. S. *J. Chem. Eng. Data* **1967**, *12*, 66.
(92) Kell, G. S. *J. Chem. Eng. Data* **1975**, *20*, 97.
(93) Harr, L.; Gallagher, J. S.; Kell, G. S. *NBS/NRC Steam Tables: Thermodynamic and Transport Properties and Computer Programs for Vapor and Liquid States of Water in SI Units*; Hemisphere Publishing Corp.: Washington, DC, 1984.
(94) Allen, M. P.; Tildesley, D. J. *Computer Simulation of Liquids*; Clarendon Press: Oxford, U.K., 1987.
(95) Steinbach, P. J.; Brooks, B. R. *J. Comput. Chem.* **1994**, *15*, 667.
(96) Prevost, M.; Van Belle, D.; Lippens, G.; Wodak, S. *Mol. Phys.* **1990**, *19*, 726.
(97) Jorgensen, W. J.; Jenson, C. *J. Comput. Chem.* **1998**, *19*, 1179.
(98) Badyal, Y. S.; Saboungi, M.-L.; Price, D. L.; Shastri, S. D.; Haeffner, D. R.; Soper, A. K. *J. Chem. Phys.* **2000**, *112*, 9206.
(99) Batista, E. R.; Xantheas, S. S.; Jónsson, H. *J. Chem. Phys*. **2000**, *112*, 3285.

(100) Silvestrelli, P. L.; Bernasconi, M.; Parrinello, M. *Chem. Phys. Lett.* **1997**, *273*, 360.
(101) Silvestralli, P. L.; Parrinello, M. *Phys. Rev. Lett.* **1999**, *82*, 3308.
(102) Kaatze, U.; Uhlendorf, Z. V. *Phys. Chem. Neue Folge* **1981**, *126*, 151.
(103) Weast, R. C., Ed. *CRC Handbook of Chemistry and Physics*; CRC Press, Boca Raton, FL, 1985−1986; Vol. 66.
(104) Tyrell, H. J. V.; Harris, K. M. *Diffusion in Liquids: A Theoretical and Experimental Study*; Butterworths: London, 1984.
(105) Krynicki, K.; Green, C. D.; Sawyer, D. W. *Faraday Discuss. Chem. Soc*. **1978**, *66*, 199.
(106) Wallqvist, A.; Astrand, P.-O. *J. Chem. Phys*. **1994**, *102*, 6559.
(107) Jedlovszky, P.; Vallauri, R. *Mol. Phys.* **1999**, *97*, 1157.
(108) Boodholt, J.; Sampoli, M.; Vallauri, R. *Mol. Phys.* **1995**, *85*, 81.
(109) Malmberg, C. G.; Maryott, A. *J. Res. Natl. Bur. Stand.* **1956**, *56*, 1.
(110) Dorsey, N. E. *Properties of Ordinary Water-Substance in All Its Phases: Water Vapor, Water, and All the Ices*; Reinhold: New York, 1940.